Critical frontier of the Potts and percolation models on triangular-type and kagome-type lattices. I. Closed-form expressions

F. Y. Wu
Department of Physics, Northeastern University, Boston, Massachusetts 02115, USA
(Received 7 February 2010; published 4 June 2010)

We consider the Potts model and the related bond, site, and mixed site-bond percolation problems on triangular-type and kagome-type lattices, and derive closed-form expressions for the critical frontier. For triangular-type lattices the critical frontier is known, usually derived from a duality consideration in conjunction with the assumption of a unique transition. Our analysis, however, is rigorous and based on an established result without the need of a uniqueness assumption, thus firmly establishing all derived results. For kagome-type lattices the exact critical frontier is not known. We derive a closed-form expression for the Potts critical frontier by making use of a homogeneity assumption. The closed-form expression is unique, and we apply it to a host of problems including site, bond, and mixed site-bond percolations on various lattices. It yields exact thresholds for site percolation on kagome, martini, and other lattices and is highly accurate numerically in other applications when compared to numerical determination.

DOI: 10.1103/PhysRevE.81.061110 PACS number(s): 05.50.+q, 02.50.−r, 64.60.Cn

I. INTRODUCTION

An outstanding problem in lattice statistics is the determination of the critical frontier, or the loci of critical point, of lattice models. Of special interest are the q-state Potts model [1] and its associated lattice models [2]. For $q=2$ it is the Ising model, and for $q=1$ the Potts model generates the percolation problem [3] including the bond [4], site [5], and mixed site-bond percolations. However, except for the simple square, triangular, and honeycomb lattices [6] and some special lattices essentially of a triangular type [7], the determination of the Potts critical frontier in general has proven to be elusive.

In this paper we consider the Potts model on two general classes of lattices: the triangular- and kagome-type lattices shown in Fig. 1. Shaded triangles in Fig. 1 denote the most general interactions involving three Potts spins $\tau_1,\tau_2,\tau_3=1,2,\ldots,q$ with the Boltzmann weights written in the form of

$$W_\Delta(1,2,3)=A+B(\delta_{12}+\delta_{23}+\delta_{31})+C\delta_{123},$$

$$W_\nabla(1,2,3)=A'+B'(\delta_{12}+\delta_{23}+\delta_{31})+C'\delta_{123}, \qquad (1)$$

where $\delta_{ij}=\delta_{\mathrm{Kr}}(\tau_i,\tau_j)$, $\delta_{123}=\delta_{12}\delta_{23}\delta_{31}$, and A,B,C,A',B',C' are constants. For shaded triangles containing additional internal Potts spins $\tau_4,\tau_5,\ldots$, for example, the constants are obtained by summing over the internal spin states. In Eqs. (1), we have assumed interactions isotropic in the three directions of a triangle. The extension of our analysis to anisotropic interactions is straightforward and will not be given.

Special cases of shaded triangles are the "stack-of-triangle" or subnet lattices shown in Figs. 2 and 3 that have been of recent interest [8–11]. We refer to these stack-of-triangle lattices as subnet lattices. The 1×1 subnet lattices are the triangular and kagome lattices themselves. We shall call a kagome-type lattice with $m\times m$ down-pointing and $n\times n$ up-pointing subnets an $(m\times m):(n\times n)$ subnet lattice or simply an $(m\times m):(n\times n)$ lattice. Examples of these kagome-type subnet lattices are shown in Fig. 3.

Partition functions for the two lattices in Fig. 1 are

$$Z_{\mathrm{tri}}(q;A,B,C)=\sum_{\tau_i=1}^{q}\prod_{\Delta}W_\Delta(i,j,k), \qquad (2)$$

$$Z_{\mathrm{kag}}(q;A,B,C;A',B',C')=\sum_{\tau_i=1}^{q}\left[\prod_{\Delta}W_\Delta(i,j,k)\right]\times\left[\prod_{\nabla}W_\nabla(i',j',k')\right], \qquad (3)$$

where the products are taken over the respective up- and down-pointing shaded triangles. The critical frontier of the triangular-type lattice in Fig. 1(a) has been known from earlier works [12–14], but the critical frontier for the kagome-type lattice in Fig. 1(b) is open.

For $q=2$, the Potts spins τ can always be replaced with Ising spins $\sigma=\pm1$ and shaded triangles with triangles (1×1 subnet) with an Ising interaction $K_I(=K/2)$. To determine K_I, we write

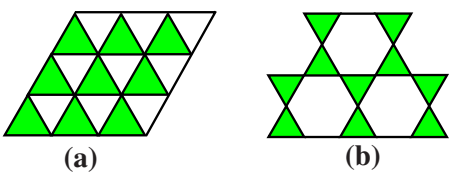

FIG. 1. (Color online) (a) Triangular-type lattice. (b) Kagome-type lattice. Shaded triangles possess Boltzmann weights (1).

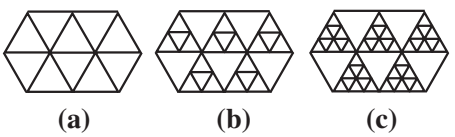

FIG. 2. Triangular subnet lattices. (a) 1×1 lattice (triangular). (b) 2×2 lattice. (c) 3×3 lattice.

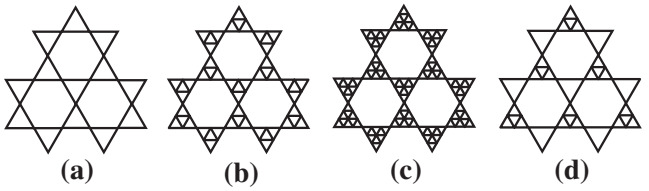

FIG. 3. Kagome subnet lattices. (a) $(1\times1):(1\times1)$ lattice (kagome). (b) $(2\times2):(2\times2)$ lattice. (c) $(3\times3):(3\times3)$ lattice. (d) $(1\times1):(2\times2)$ lattice.

$$\delta_{ij} = \tfrac{1}{2}(1+\sigma_i\sigma_j),$$

$$W_\Delta(1,2,3) = \exp[2K_I(\delta_{12}+\delta_{23}+\delta_{31})]. \tag{4}$$

Equating Eqs. (4) with W_Δ in Eq. (1), one obtains after a little algebra

$$e^{4K_I} = (A+3B+C)/(A+B). \tag{5}$$

It follows that the partition functions (2) and (3) are completely equivalent to those of the triangular and kagome Ising models.

For $q\geq3$, the shaded triangles can be replaced with any triangular network having two independent parameters. An example is the mapping shown in Fig. 12 in Sec. III G.

Parameters A,B,C for given $n\times n$ Potts subnets can be readily worked out. For the 1×1 triangle, for example, one has

$$W_\Delta(1,2,3) = \exp[K(\delta_{12}+\delta_{23}+\delta_{31})], \tag{6}$$

from which one obtains

$$A=1, \quad B=v, \quad C=3v^2+v^3 \quad \text{(triangle)}, \tag{7}$$

where $v=e^K-1$. For the 2×2 subnet, one obtains in a similar fashion

$$A = 3v^5+21v^4+(50+4q)v^3+33qv^2+9q^2v+q^3,$$

$$B = v^7+7v^6+22v^5+(30+2q)v^4+10qv^3+q^2v^2,$$

$$C = v^9+9v^8+33v^7+63v^6+(54+3q)v^5+9qv^4 \quad (2\times2 \text{ subnet}). \tag{8}$$

Expressions of A,B,C for $n\times n$ subnets up to $n=7$ are derived and given in the subsequent paper [15], hereafter referred to as paper II [15].

The structure of this paper is as follows. In Sec. II we consider the triangular subnet lattices and apply the rigorously known critical frontier to various models including mixed site-bond percolation. In Sec. III we consider the kagome-type lattice and derive a closed-form expression for its critical frontier on the basis of a homogeneity assumption. We show that this critical frontier is exact for site percolation on the kagome, martini, and other lattices and is highly accurate in other applications. The accuracy of the critical frontier will be closely examined in paper II [15].

II. TRIANGULAR-TYPE LATTICES

In this section we consider triangular-type lattices in Fig. 1(a). The Potts model on the triangular-type lattice was first studied by Baxter *et al.* [12] in the context of a Potts model with two- and three-site interactions. Using a Bethe-ansatz result on a 20-vertex model on the triangular lattice due to Kelland [16,17], they showed that the partition function (2) is self-dual and derived its self-dual point which, in the language of interaction (1), reads

$$qA = C. \tag{9}$$

This self-dual trajectory was later rederived graphically by Wu and Lin [13]. However, as is common in duality arguments, an additional assumption of a unique transition is needed to ascertain that Eq. (9) is indeed the actual critical frontier.

However, Wu and Zia [14] established subsequently in a rigorous analysis that Eq. (9) is indeed the critical frontier in the "ferromagnetic" regime,

$$2B+C>0, \quad 3B+C>0. \tag{10}$$

It can be verified that condition (10) holds for Eqs. (7) and (8), so the critical frontier $qA=C$ is exact. Applications of Eq. (9) to the martini and other lattices have been reported in [7]. The duality relation of the triangular Potts model with two- and three-spin interactions has also be studied by Chayes and Lei [18] with several rigorous theorems on the phase transition proven.

A. Ising model

In Sec. I, we have established that for $q=2$ any triangular-type lattice is reducible to a triangular Ising lattice with interaction K_I given by Eq. (5). Indeed, using Eq. (5), the known critical point $e^{4K_I}=3$ of the triangular Ising model reduces to the critical frontier $2A=C$ as expected.

For the Ising model on 1×1 and 2×2 subnet lattices with interaction K_I, we set $q=2$, $v=e^{2K_I}-1$ in Eqs. (7) and (8) and obtain from $2A=C$ the critical point

$$x_c = \sqrt{3}, \quad 1\times1 \text{ subnet (triangular lattice)}$$

$$= \sqrt{5}, \quad 2\times2 \text{ subnet}, \tag{11}$$

where $x=e^{2K_I}$. Using expressions of A and C given in paper II [15] for 3×3 and 4×4 subnets, we obtain similarly

$$x^8-5x^6-x^4-19x^2-8=0,$$

$$x_c = \tfrac{1}{2}\sqrt{5+\sqrt{33}+\sqrt{(50+18\sqrt{33})}} = 2.404\,689\,372, \quad 3\times3 \text{ subnet},$$

$$x^{12}-5x^{10}-x^8-22x^6-53x^4-125x^2-51=0,$$

$$x_c = 2.467\,648\,033, \quad 4\times4 \text{ subnet}. \tag{12}$$

B. Bond percolation

It is well known that bond percolation is realized in the $q=1$ limit of the Potts model under the mapping $v=p/$

TABLE I. Exact Potts threshold e^{K_c} for triangular-type subnet lattices.

	$q=1$	$q=2$ (Ising)	$q=3$	$q=4$	$q=10$
Triangular lattice	1.532088885	$\sqrt{3}$	1.879385241	2	2.492033301
2×2	1.892608790	$\sqrt{5}$	2.493123120	2.706275430	3.602637947
3×3	2.036982609	2.404689372	2.674398828	2.895419068	3.808005450
4×4	2.102451724	2.467648033	2.731876784	2.946645097	3.820754228

$(1-p)$, where p is the bond occupation probability [3,4]. Therefore, the percolation threshold is given simply by $C=A$. Thus, using Eq. (7) for A and C for the triangular lattice, one obtains the well-known [19–21] critical frontier for bond percolation,

$$1-3p+p^3=0 \quad \text{or} \quad p_c=2\sin(\pi/18) = 0.347\,296\,355 \quad \text{(triangular lattice)}. \tag{13}$$

For the 2×2 subnet lattice we use Eqs. (8) and obtain

$$1-3p^2-9p^3+3p^4+45p^5-72p^6+45p^7-12p^8+p^9=0,$$

$$\text{or} \quad p_c=0.471\,628\,788 \quad (2\times2 \text{ subnet lattice}). \tag{14}$$

In a similar fashion using expressions of A and C given in paper II [15], we obtain

$$1-3p^3-18p^4-39p^5+77p^6+309p^7-198p^8-1406p^9+315p^{10}+9303p^{11}-23\,083p^{12}+28\,707p^{13}-22\,047p^{14}+10\,959p^{15}-3462p^{16}+636p^{17}-52p^{18}=0,$$

$$p_c=0.509\,077\,792 \quad (3\times3 \text{ subnet lattice}), \tag{15}$$

$$1-3p^4-30p^5-114p^6-63p^7+636p^8+1940p^9+741p^{10}-14\,283p^{11}-26\,541p^{12}+78\,759p^{13}+18\,9279p^{14}-370\,589p^{15}-1\,229\,877p^{16}+2\,829\,339p^{17}+6\,938\,691p^{18}-41\,655\,363p^{19}+96\,750\,306p^{20}-143\,421\,123p^{21}+152\,405\,700p^{22}-121\,438\,416p^{23}+73\,822\,093p^{24}-34\,270\,647p^{25}+11\,994\,555p^{26}-3\,073\,478p^{27}+545\,409p^{28}-60\,012p^{29}+3089p^{30}=0,$$

$$p_c=0.524\,364\,822 \quad (4\times4 \text{ subnet lattice}). \tag{16}$$

These findings agree with those of Haji-Akbari and Ziff [11] deduced from a duality consideration. As aforementioned, our derivation now ascertains that these thresholds are the exact transition points.

C. Potts model

The exact critical threshold for the Potts model on triangular-type lattices is Eq. (9), or $qA=C$. Using expressions of A and C given in Eq. (7), one obtains the known critical frontier [6,22]

$$3v^2+v^3=q \quad \text{(Potts model on triangular lattice)}. \tag{17}$$

For the 2×2 subnet lattice one uses Eqs. (8) and obtains the critical frontier

$$v^9+9v^8+33v^7+63v^6+54v^5-12qv^4-(50q+4q^2)v^3-33q^2v^2-9q^3v-q^4=0. \tag{18}$$

Solutions of Eqs. (17) and (18) and those of the 3×3 and 4×4 subnet lattices using expressions of A and C given in paper II [15] are tabulated in Table I for $q=1,2,3,4,10$. Note that the $q=1$ solutions are related to the bond percolation thresholds (13)–(16) by $e^{K_c}=1/(1-p_c)$.

D. Site percolation

Kunz and the present author [5] showed that site percolation can be formulated as a $q=1$ limit of a Potts model with multisite interactions. The Kunz-Wu scheme is to consider a *reference* lattice with multispin interactions and regard faces of multispin interactions as sites of a new lattice on which the site percolation is defined. The critical frontier of the Potts model on the reference lattice then produces the site percolation threshold for the new lattice. This scheme of formulation can be extended to mixed site-bond percolation.

1. Site percolation on the triangular lattice

Consider as a reference lattice the triangular lattice with pure three-site interactions M marked by dots shown in the left panel of Fig. 4. The dots form a triangular lattice shown in the right. The Kunz-Wu scheme now solves the site percolation on the triangular lattice. We have

$$W_\Delta(1,2,3)=e^{M\delta_{123}}=1+m\delta_{123}, \tag{19}$$

or $A=1$, $B=0$, $C=m=e^M-1$. Writing $m=s/(1-s)$, where $s=1-e^{-M}$ is the site occupation probability, the exact critical

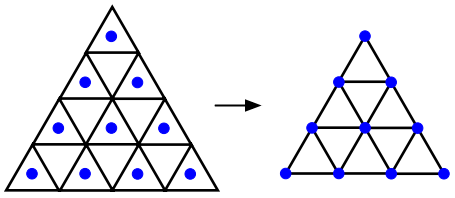

FIG. 4. (Color online) Site percolation on the triangular lattice.

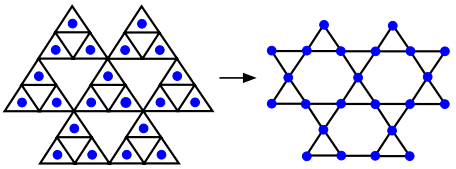

FIG. 5. (Color online) Site percolation on the kagome lattice.

frontier $A=C$ now yields immediately the well-known site percolation threshold [19–21,23] for the triangular lattice,

$$s_c = 1/2. \tag{20}$$

2. Site percolation on kagome lattice

Consider the reference 2×2 subnet lattice with pure three-site interactions M denoted by dots shown in the left panel of Fig. 5. The Kunz-Wu scheme then maps the reference Potts model into site percolation on the kagome lattice as indicated in the right.

Now for a 2×2 subnet containing three dots as in Fig. 5, we have

$$A = q^3 + 3qm, \quad B = m^2, \quad C = m^3, \tag{21}$$

where $m=e^M-1$. Writing $m=s/(1-s)$ and setting $q=1$, the rigorous critical frontier $A=C$ yields the critical condition $1-3s^2+s^3=0$, leading to the known exact result [19,20]

$$s_c^{kag} = 1 - 2\sin(\pi/18) = 0.652\,703\,644. \tag{22}$$

3. Site percolation on $(1\times 1):(n\times n)$ lattices

The above scheme of mapping can be extended to site percolation on $(1\times 1):(n\times n)$ lattices for general n. The example in Fig. 5 is $n=1$, and the $n=2$ lattice is shown in Fig. 6. The reference lattice (not shown) for $n=2$ consists of 3×3 subnets with

$$A = q^7 + 6q^5m + 15q^3m^2 + (14q + 3q^2)m^3 + 3m^4,$$

$$B = q^2m^3 + 2(q+1)m^4 + m^5,$$

$$C = 3m^5 + m^6, \tag{23}$$

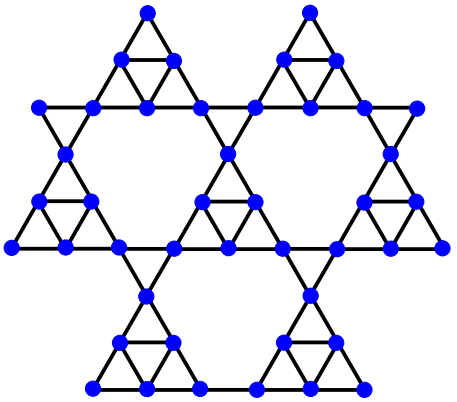

FIG. 6. (Color online) Site percolation on the $(1\times 1):(2\times 2)$ lattice.

where $m=e^M-1$ and M is the three-site interaction. After setting $q=1$ and $m=s/(1-s)$, the critical frontier $qA=C$ becomes

$$(1-2s^2)(1+2s^2-3s^3+s^4) = 0, \tag{24}$$

yielding the exact threshold

$$s_c = 1/\sqrt{2}, \quad (1\times 1):(2\times 2) \text{ kagome site percolation}. \tag{25}$$

The exact critical threshold for higher $(1\times 1):(n\times n)$ lattices can be similarly worked out. Results for up to $n=6$ are tabulated in Table VII of paper II [15].

III. KAGOME-TYPE LATTICES

We consider in this section the case of the kagome-type lattices in Fig. 1(b). The critical frontier of the Potts model on kagome-type lattices has proven to be highly elusive. On the basis of a homogeneity assumption, however, the present author [6] has advanced a conjecture on the critical point for the kagome lattice. The conjecture has since been closely examined [24–27] and found to be extremely accurate. Here, we extend the homogeneity assumption to general kagome-type Potts lattices. For continuity of reading, we first state our result in Sec. III A and present the derivation in Sec. III G.

A. Closed-form critical frontier and homogeneity assumption

For Potts model on kagome-type lattices described by the partition function (3), the critical frontier under a homogeneity assumption is

$$(q^2A + 3qB + C)(q^2A' + 3qB' + C') - 3(qB + C)(qB' + C') - (q-2)CC' = 0. \tag{26}$$

Remarks:

(1) Despite its appearance, the critical frontier (26) actually contains only three independent parameters [cf. Eqs. (55) below].

(2) Expression (26) is exact for $q=2$.

B. Ising model

We first show that Eq. (26) is exact for $q=2$. We have already established that the partition function (3) is precisely that of the kagome Ising model. For completeness we now verify that the critical frontier (26) also gives the known kagome critical point.

For symmetric weights $A=A'$, $B=B'$, $C=C'$, the kagome Ising model has a uniform interaction K_I and the critical point is known to be at $e^{4K_I}=3+2\sqrt{3}$ [28]. It is readily verified that, by using Eq. (5) for K_I, this critical point gives rise to precisely the $q=2$ critical frontier (26), namely,

$$4A + 6B + C = \sqrt{3}(2B + C). \tag{27}$$

The proof can be extended to the kagome-type model with asymmetric weights.

TABLE II. Bond percolation threshold p_c for $(m\times m):(n\times n)$ lattices for $m,n\leq 4$.

Lattice	This work	Numerical determination
Kagome	0.524429717	0.52440499(2) [27]
$(1\times 1):(2\times 2)$	0.570882620	0.57086651(33) [29]
$(1\times 1):(3\times 3)$	0.599798340	
$(1\times 1):(4\times 4)$	0.592017120	
$(2\times 2):(2\times 2)$	0.600870248	0.6008624(10) [10]
$(2\times 2):(3\times 3)$	0.610916740	
$(2\times 2):(4\times 4)$	0.614703624	
$(3\times 3):(3\times 3)$	0.619333485	0.6193296(10) [10]
$(3\times 3):(4\times 4)$	0.622473191	
$(4\times 4):(4\times 4)$	0.625364661	0.625365(3) [10]

Critical thresholds of kagome-type Ising subnet lattices computed from Eq. (27) are tabulated in Table III. For the kagome and $(2\times 2):(2\times 2)$ Ising lattices, for example, we use Eqs. (7) and (8) for A,B,C with $q=1$, $v=x-1$, $x=e^{2K_I}$. This gives

$$x^4-6x^2-3=0,$$

$$x_c=\sqrt{3+2\sqrt{3}}=2.542\,459\,756 \quad \text{(kagome lattice)},$$

$$x^8-8x^6-6x^4-32x^2-83=0,$$

$$x_c=\sqrt{2+\sqrt{3}+\sqrt{12+10\sqrt{3}}}=3.024\,382\,957, \quad (2\times 2):(2\times 2) \text{ lattice}. \tag{28}$$

C. Bond percolation

For bond percolation threshold on kagome-type subnet lattices, we again use Eq. (26) with the substitution of $q=1$ and $v=p/(1-p)$, where p is the bond occupation probability. Using Eqs. (7) and (8), we obtain

$$1-3p^2-6p^3+12p^4-6p^5+p^6=0,$$

$$p_c=0.524\,429\,717 \quad \text{(kagome lattice)}, \tag{29}$$

$$1-3p^3-12p^4-12p^5+63p^6+60p^7-330p^8+423p^9-264p^{10}+84p^{11}-11p^{12}=0,$$

$$p_c=0.570\,882\,620, \quad (1\times 1):(2\times 2) \text{ lattice}, \tag{30}$$

$$1-3p^4-18p^5-39p^6+30p^7+273p^8+264p^9-1785p^{10}-126p^{11}+8232p^{12}-16\,236p^{13}+16\,359p^{14}-9948p^{15}+3708p^{16}-786p^{17}+73p^{18}=0,$$

$$p_c=0.600\,870\,248, \quad (2\times 2):(2\times 2) \text{ lattice}. \tag{31}$$

Bond percolation thresholds computed from Eq. (26) for $(m\times m):(n\times n)$ lattices are tabulated in Table II. We also include in Table II numerical determinations of p_c for the $(1\times 1):(2\times 2)$ [29] and $(n\times n)\times(n\times n)$, where $n=2,3,4$ [10], lattices by Ziff and Gu using simulations, and of the kagome lattice by Feng *et al.* [27] from a transfer matrix analysis. The comparison shows that Eq. (26) is accurate to within one part in 10^5.

D. Potts model

Critical thresholds for the Potts model on kagome-type subnet lattices computed from Eq. (26) are tabulated in Table III. For the kagome lattice itself, for example, we have $A=A'=1$, $B=B'=v$, $C=C'=3v^2+v^3$, $v=e^K-1$, and Eq. (26) gives the critical frontier

$$v^6+6v^5+9v^4-2qv^3-12qv^2-6q^2v-q^3=0 \quad \text{(kagome lattice)}. \tag{32}$$

The critical frontier (32) for the kagome lattice was first obtained by the present author some 30 years ago [6,30] by using the homogeneity assumption described in Sec. III G. Comparison of the thresholds computed from Eq. (32) for $q=1,3,4$ with Monte Carlo renormalization-group findings has shown that the accuracy of Eq. (26) is within one part in 10^5 [24].

TABLE III. Potts threshold e^{K_c} for kagome-type subnet lattices.

Lattice	$q=1$	$q=2$ (Ising)	$q=3$	$q=4$	$q=10$
Kagome lattice	2.102738619	2.542459757	2.876269226	3.155842236	4.355385241
$(1\times 1):(2\times 2)$	2.330364713	2.821281889	3.186678923	3.489096458	4.761529399
$(1\times 1):(3\times 3)$	2.498740260	2.903273662	3.260483758	3.553390863	4.764908410
$(1\times 1):(4\times 4)$	2.451083242	2.928442860	3.276998285	3.562314883	4.739553252
$(2\times 2):(2\times 2)$	2.505450909	3.024382957	3.481055307	3.717691692	5.016332520
$(2\times 2):(3\times 3)$	2.570143984	3.082166484	3.454087416	3.757519846	5.004155712
$(2\times 2):(4\times 4)$	2.595404635	3.098624716	3.378293046	3.761399505	4.984524206
$(3\times 3):(3\times 3)$	2.626971274	3.133002727	3.497087416	3.712498867	4.992841134
$(3\times 3):(4\times 4)$	2.648818511	3.147204863	3.416364328	3.796037357	4.973931010
$(4\times 4):(4\times 4)$	2.669262336	3.160721132	3.598289910	3.639241821	4.954642401

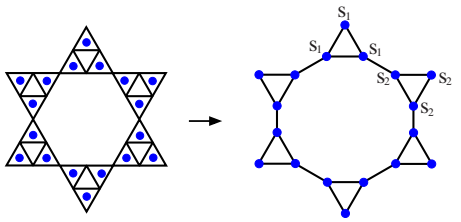

FIG. 7. (Color online) Site percolation on the 3-12 lattice.

E. Site and site-bond percolations

We now apply Eq. (26) to site as well as mixed site-bond percolation. First we show that Eq. (26) is exact in some instances.

1. Site percolation on the 3-12 and kagome lattices

The 3-12 lattice is the lattice shown in the right panel of Fig. 7. To formulate site percolation on the 3-12 lattice, we consider the reference $(2\times2):(2\times2)$ lattice with pure three-site interactions shown in the left. Let the three-site interactions of the up and down triangles be, respectively, M_1 and M_2. One finds

$$A = q^3 + 3qm_1, \quad B = m_1^2, \quad C = m_1^3,$$

$$A' = q^3 + 3qm_2, \quad B' = m_2^2, \quad C' = m_2^3, \tag{33}$$

where $m_1=e^{M_1}-1$ and $m_2=e^{M_2}-1$. Setting $q=1$, $m_1=s_1/(1-s_1)$, and $m_2=s_2/(1-s_2)$, where s_1 and s_2 are the respective site occupation probabilities for the 3-12 lattice, the critical frontier (26) gives

$$1-3(s_1s_2)^2+(s_1s_2)^3=0 \quad \text{(3-12 site percolation)}. \tag{34}$$

For $s_1=s_2=s$, this yields the known [19,23] critical frontier $1-3s^4+s^6=0$ or

$$s_c^{3\text{-}12}=\sqrt{1-2\sin(\pi/18)}=0.807\,900\,076. \tag{35}$$

Using the relation $s_c^{kag}=(s_c^{3\text{-}12})^2$ [23], we have therefore derived the exact kagome and 3-12 site percolation thresholds and demonstrated that Eq. (26) is exact in this instance.

2. Site percolation on the martini lattice

The martini lattice [31] is the lattice shown in the right panel of Fig. 8. To generate a site percolation on the martini lattice, we start from the $(1\times1):(2\times2)$ reference lattice with three-site interactions shown in the left. Denote the three-site interactions of up- and down-pointing triangular faces by M_1 and M_2, respectively, and write $m_1=e^{M_1}-1$ and $m_2=e^{M_2}-1$. We have

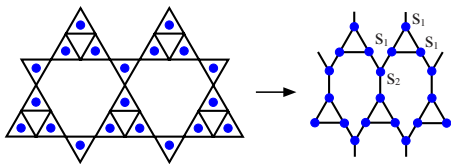

FIG. 8. (Color online) Site percolation on the martini lattice.

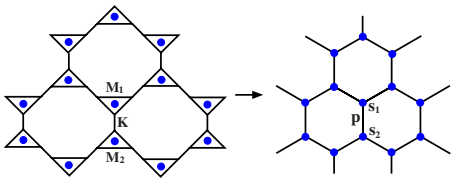

FIG. 9. (Color online) Site-bond percolation on the honeycomb lattice.

$$A = q^3 + 3qm_1, \quad B = m_1^2, \quad C = m_1^3,$$

$$A' = 1, \quad B' = 0, \quad C' = m_2. \tag{36}$$

Setting $q=1$ and $m_1=s_1/(1-s_1)$, $m_2=s_2/(1-s_2)$, with s_1 and s_2 as the respective site occupation probabilities, Eq. (26) gives the critical frontier

$$1-(3s_1^2-s_1^3)s_2=0 \quad \text{(martini site percolation)}. \tag{37}$$

This is a known exact result [26,32,33] and is another example that the critical frontier Eq. (26) is exact. For $s_2=1$, the percolation reduces to that on the kagome lattice, and Eq. (37) gives the threshold (22). For uniform occupation probability $s_1=s_2=s$, Eq. (37) becomes $1-3s^3+s^4=0$ and gives the exact solution $s_c^{martini}=0.764\,826\,486$.

3. Site-bond percolation on the honeycomb lattice

No exact result is known for the site and site-bond percolations on the honeycomb lattice. Owing to the intrinsic interest of a percolation process on a simple lattice, the problem of honeycomb site percolation has attracted considerable attention for many years. There now exists a host of highly precise numerical estimates on the threshold for site percolation on the honeycomb lattice [10,23,27].

Consider the more general mixed site-bond percolation on the honeycomb lattice with site occupation probabilities s_1 and s_2 and bond occupation probability p shown in the right panel of Fig. 9. The relevant reference lattice can be taken as shown in the left with edge interactions K and three-site interactions M_1 and M_2. To make use of Eq. (26), we adopt the scheme of devising up- and down-pointing triangles as indicated in Fig. 11(b) below. This gives

$$A = (q+v)^3 + (q+3v)m_2, \quad B = v^2m_2, \quad C = v^3m_2,$$

$$A' = 1, \quad B' = 0, \quad C' = m_1, \tag{38}$$

where $v=e^K-1$, $m_i=e^{M_i}-1$, $i=1,2$. Setting $q=1$, $v=p/(1-p)$, $m_i=s_i/(1-s_i)$, we obtain from Eq. (26) the critical frontier for the mixed site-bond percolation as

$$(3p^2-p^3)s_1s_2=1 \quad \text{(honeycomb site-bond percolation)}. \tag{39}$$

When $s_1=s_2=1$, Eq. (39) is exact since it gives the known honeycomb bond percolation threshold $1-3p^2+p^3=0$ [19–21]. When $p=1$, Eq. (39) gives the threshold

$$s_1s_2=1/2, \tag{40}$$

which is exact for $s_2=1$, as the site percolation reduces to one on the triangle lattice with the critical point (20), s_c

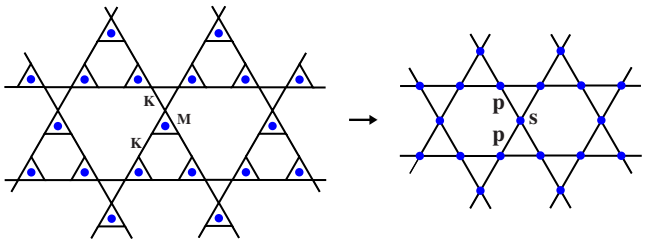

FIG. 10. (Color online) Site-bond percolation on the kagome lattice.

$=1/2$. But for $s_1=s_2=s$, Eq. (40) gives $s_c=1/\sqrt{2}=0.707\ 106\ 781$ differing from accurate numerical estimates of $s_c=0.697\ 040\ 2$ [27] and $s_c=0.697\ 041\ 3$ [10]. The critical frontier (26) is therefore a close approximation in this instance.

The site-bond percolation has also been studied by simulations by Ziff and Gu for $s_1=s_2$ [10] and for $p=1$ [29]. Their results indicate that Eq. (39) works better for site occupation probabilities ~ 1.

4. Site-bond percolation on the kagome lattice

Consider the mixed site-bond percolation on the kagome lattice with site and bond occupation probabilities s and p shown in the right panel of Fig. 10. The reference lattice is shown in the left having edge interaction K and three-site interaction M. Regard the reference lattice as a kagome type with the partition function (3). One has

$$A = q(q^2+3m)(q+v)^3 + 3m^2(q+v)^2 + m^3,$$

$$B = m^2(q+v)^2 + m^3 v,$$

$$C = m^3(3v^2+v^3),$$

$$A'=1, \quad B'=v, \quad C'=3v^2+v^3, \tag{41}$$

where $v=e^K-1$, $m=e^M-1$. Substituting Eq. (41) into Eq. (26) and setting $q=1$, $v=p/(1-p)$, $m=s/(1-s)$, one obtains the critical frontier

$$1+3s^2(1-3p+2p^3-p^4)+s^3(-3+9p-3p^2-12p^3+15p^4 - 6p^5+p^6)=0 \quad \text{(kagome site-bond percolation)}. \tag{42}$$

For $p=1$, Eq. (42) becomes $1-3s^2+s^3=0$, which gives the exact critical threshold (22) for the kagome site percolation. For $s=1$, Eq. (42) becomes $1-3p^2-6p^3+12p^4-6p^5+p^6=0$ or $p_c=0.524\ 429\ 717$, in agreement with Eq. (29).

F. 3-12 lattice

The 3-12 lattice is the lattice shown in Fig. 11(a) with interactions K, K_1, K_2. To make use of (26) we regard the lattice as one of the kagome type consisting of large up-pointing triangles (dotted lines) and small down-pointing triangles as indicated in Fig. 11(b). Then we have (see also Eq. (5) of [7])

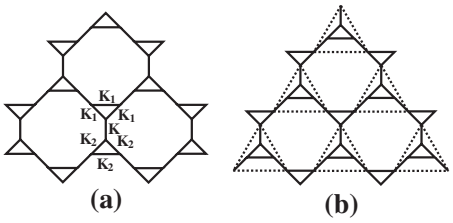

FIG. 11. (a) The 3-12 Potts lattice. (b) The 3-12 lattice as an asymmetric kagome-type lattice.

$$A = (q+v)^3 + 3(q+v)(q+2v)v_2 + 3(q+3v)v_2^2 + (q+3v)v_2^3,$$

$$B = v^2[(q+v)v_2 + 3v_2^2 + v_2^3],$$

$$C = v^3(3v_2^2+v_2^3),$$

$$A'=1, \quad B'=v_1, \quad C'=3v_1^2+v_1^3, \tag{43}$$

where $v=e^K-1$, $v_1=e^{K_1}-1$, $v_2=e^{K_2}-1$. Substituting Eq. (43) into Eq. (26), we obtain the critical frontier (rearranged in a symmetric form)

$$(q+v)^3(h_1+3qv_1+q^2)(h_2+3qv_2+q^2) - 3(qv^2+v^3)(h_1 + qv_1)(h_2+qv_2) - (q-2)v^3h_1h_2 = 0, \tag{44}$$

where $h_i=3v_i^2+v_i^3$, with $i=1,2$.

For the 3-12 Ising model with uniform interactions K_I, we set $q=2$ and $v_1=v_2=v=e^{2K_I}-1$, and Eq. (44) simplifies to

$$(\sqrt{3}-1)v^2 - 2v - 4 = 0, \tag{45}$$

yielding the known exact critical point $e^{2K_I}=\frac{1}{2}(3+\sqrt{3})+\sqrt{(6+5\sqrt{3})/2}=5.073\ 446\ 135$ in agreement with Utiyama [34] and Syozi [28].

For Potts model on the 3-12 lattice with uniform interaction K, Eq. (44) gives

$$v^9+6v^8+3(3-q)v^7-q(32+q)v^6-q(75+30q)v^5-q^2(111 + 12q)v^4-2q^3(41+q)v^3-36q^4v^2-9q^5v-q^6=0. \tag{46}$$

This gives the critical point

$$e^{K_c}=v+1=3.852\ 426\ 158, \quad q=1$$

$$=5.073\ 446\ 135, \quad q=2 \quad \text{(exact Ising result)}$$

$$=6.033\ 022\ 515, \quad q=3$$

$$=6.857\ 394\ 828, \quad q=4. \tag{47}$$

The accuracy of prediction (47) will be examined in paper II [15].

For bond percolation on the 3-12 lattice we set $q=1$ and write $v=p/(1-p)$, $v_1=p_1/(1-p_1)$, $v_2=p_2/(p_2-p_2)$, where p, p_1, p_2 are the respective bond occupation probabilities. Then Eq. (44) gives the critical frontier

$$1-3p^2(p_1+p_1^2-p_1^3)(p_2+p_2^2-p_2^3)+p^3(3p_1^2-2p_1^3)(3p_2^2 - 2p_2^3)=0 \quad \text{(3-12 bond percolation)}. \tag{48}$$

This expression has been conjectured recently by Scullard

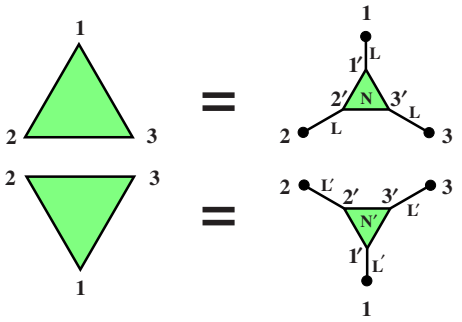

FIG. 12. (Color online) Graphical representation of Eq. (52).

and Ziff [26] as a nonrigorous extension of the exact bond percolation threshold of the martini lattice. In the uniform case $p_1=p_2=p$, Eq. (48) becomes

$$1-p+p^2+p^3-7p^4+4p^5=0, \quad p_c=0.740\,423\,317, \tag{49}$$

which is also given by $p_c=1-e^{-K_c}$ using e^{K_c} for $q=1$ in Eq. (47). Compared to the numerical determination of $p_c=0.740\,421\,95(80)$ by Ziff and Gu [10] and the value $p_c=0.740\,420\,81$ by Parviainen [35], the accuracy of the homogeneity determination (49) is seen to be well within one part in 10^5.

For the mixed site-bond percolation on the 3-12 lattice, it is tempting to use the kagome critical frontier (42) and replace s with s^2p as argued by Suding and Ziff [23]. This gives the critical frontier

$$1+3s^4(p-3p^2+2p^4-p^5)+s^6(-3p^3+9p^4-3p^5-12p^6 +15p^7-6p^8+p^9)=0. \tag{50}$$

For $p=1$ the pure site percolation, this becomes $1-3s^2+s^6=0$, which is exact. For $s=1$ the pure bond percolation, Eq. (50) gives

$$1+3p^2-12p^3+9p^4+3p^5-15p^6+15p^7-6p^8+p^9=0, \tag{51}$$

with the solution $p_c=0.747\,882\,617$. The small difference between Eqs. (49) and (51) reflects the approximate nature of the kagome site-bond critical frontier (42).

G. Critical frontier and homogeneity assumption

We now derive the critical conjecture (26) using a homogeneity assumption. In the partition function (2), we replace the two Boltzmann weights with

$$W_\Delta(1,2,3)=F\sum_{s_1',s_2',s_3'=1}^{q} e^{L(\delta_{11'}+\delta_{22'}+\delta_{33'})}e^{N\delta_{1'2'3'}},$$

$$W_\nabla(1,2,3)=F'\sum_{s_1',s_2',s_3'=1}^{q} e^{L'(\delta_{11'}+\delta_{22'}+\delta_{33'})}e^{N'\delta_{1'2'3'}}, \tag{52}$$

as indicated graphically in Fig. 12. Equating Eqs. (52) with Eqs. (1), we find

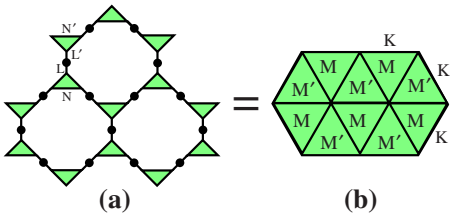

FIG. 13. (Color online) (a) The kagome-type lattice after transformation (52). (b) The lattice dual to (a).

$$A=F[(q+\ell)^3+(q+3\ell)n],$$

$$B=F\ell^2n,$$

$$C=F\ell^3n, \tag{53}$$

where $\ell=e^L-1$, $n=e^N-1$ and similar relations for A',B',C' with $\{F,\ell,n\}\to\{F',\ell',n'\}$ and $\ell'=e^{L'}-1$, $n'=e^{N'}-1$.

Solving Eq. (53) for ℓ,n,F, one obtains

$$\ell=\frac{C}{B},$$

$$n=\frac{(qB+C)^3}{AC^2-qB^3-3B^2C},$$

$$F=\frac{B^3(AC^2-qB^2-3B^2C)}{C^2(qB^2+C)^3}, \tag{54}$$

and similarly one obtains ℓ',n',F' in terms of A',B',C'. The kagome-type lattice now becomes the one shown in Fig. 13(a).

The duality relation of Potts models with multisite interactions has been formulated by Essam [21] (see also [2]). Following Essam, the dual to the lattice in Fig. 13(a) is the one shown in Fig. 13(b) with

$$e^K=(1+q/\ell)(1+q/\ell'),$$

$$e^M=1+q^2/n,$$

$$e^{M'}=1+q^2/n', \tag{55}$$

where the interaction K is the dual to the two interactions L and L' in series. We therefore are led to consider the Potts model on the triangular lattice shown in Fig. 13(b), where M and M' are three-site interactions.

For $M'=0$, the partition function is $Z_{\rm tri}(q;A,B,C)$ given by Eq. (2) with

$$W_\Delta(1,2,3)=e^{K(\delta_{12}+\delta_{23}+\delta_{31})}e^{M\delta_{123}},$$

or

$$A=1, \quad B=e^K-1, \quad C=e^{3K+M}-3e^K+2. \tag{56}$$

The exact critical frontier in this case is known. It is $qA=C$, or

$$e^{3K+M} - 3e^{K} + 2 = q. \tag{57}$$

For $M' \neq 0$ the critical frontier is not known. However, the critical frontier must be symmetric in M and M'. We now make a *homogeneity assumption* requiring M and M' to appear homogeneously in the exponent of Eq. (57). The simplest way to do this is to extend Eq. (57) to

$$e^{3K+M+M'} - 3e^{K} + 2 = q. \tag{58}$$

The substitution of expressions of K, M, and M' in Eqs. (55) and (54) into Eq. (57) now leads to Eq. (26).

IV. SUMMARY

We have considered the q-state Potts model and the related bond, site, and mixed site-bond percolations for triangular- and kagome-type lattices. For triangular-type lattices we obtained its exact critical frontier in the form of Eq. (9) without the usual assumption of a unique transition. We then applied the exact critical frontier in various applications. For kagome-type lattices we obtained a critical frontier (26) by making use of a homogeneity assumption. We established that the present critical frontier is exact for $q=2$ and for site percolation on the kagome, martini, and other lattices. For the Potts and bond percolation models for which there is no exact solution, the present critical frontier gives numerical values of critical thresholds accurate to the order of 10^{-5}. For mixed site-bond percolation, the homogeneity assumption gives rise to critical frontiers which are accurate when site occupation probabilities are ~ 1.

In summary, we emphasize that applications of the critical frontiers (9) and (26) are not limited to those reported in this paper. They can be extended to numerous other lattice models having a triangular or kagome symmetry, and thus they open the door to a host of previously unsolved problems.

ACKNOWLEDGMENTS

I would like to thank Chengxiang Ding for help in the preparation of the manuscript and Wenan Guo for a critical reading. I am grateful to R. M. Ziff for helpful comments and suggestions, and for communicating on results prior to publication.

[1] R. B. Potts, Proc. Cambridge Philos. Soc. **48**, 106 (1952).
[2] F. Y. Wu, Rev. Mod. Phys. **54**, 235 (1982).
[3] F. Y. Wu, J. Stat. Phys. **18**, 115 (1978).
[4] P. W. Kasteleyn and C. M. Fortuin, J. Phys. Soc. Jpn. **26**, 11 (1969).
[5] H. Kunz and F. Y. Wu, J. Phys. C **11**, L1 (1978); **11**, L357 (1978).
[6] F. Y. Wu, J. Phys. C **12**, L645 (1979).
[7] F. Y. Wu, Phys. Rev. Lett. **96**, 090602 (2006).
[8] D.-X. Yao, Y. L. Loh, E. W. Carlson, and M. Ma, Phys. Rev. B **78**, 024428 (2008).
[9] Y. L. Loh, D.-X. Yao, and E. W. Carlson, Phys. Rev. B **78**, 224410 (2008).
[10] R. M. Ziff and H. Gu, Phys. Rev. E **79**, 020102(R) (2009).
[11] A. Haji-Akbari and R. M. Ziff, Phys. Rev. E **79**, 021118 (2009).
[12] R. J. Baxter, H. N. V. Temperley, and S. E. Ashley, Proc. R. Soc. London, Ser. A **358**, 535 (1978).
[13] F. Y. Wu and K. Y. Lin, J. Phys. A **13**, 629 (1980).
[14] F. Y. Wu and R. K. P. Zia, J. Phys. A **14**, 721 (1981).
[15] C.-X. Ding, Z. Fu, W.-A. Guo, and F. Y. Wu, Phys. Rev. E **81**, 061111 (2010).
[16] S. B. Kelland, Aust. J. Phys. **27**, 813 (1974).
[17] S. B. Kelland, J. Phys. A **7**, 1907 (1974).
[18] L. Chayes and H. K. Lei, J. Stat. Phys. **122**, 647 (2006).
[19] M. F. Sykes and J. W. Essam, J. Math. Phys. **5**, 1117 (1964).
[20] J. W. Essam, in *Phase Transitions and Critical Phenomena*, edited by C. Domb and M. S. Green (Academic, New York, 1972), Vol. 2.
[21] J. W. Essam, J. Math. Phys. **20**, 1769 (1979).
[22] D. Kim and R. J. Joseph, J. Phys. C **7**, L167 (1974).
[23] P. N. Suding and R. M. Ziff, Phys. Rev. E **60**, 275 (1999).
[24] C. Chen, C. K. Hu, and F. Y. Wu, J. Phys. A **31**, 7855 (1998).
[25] R. M. Ziff and P. N. Suding, J. Phys. A **30**, 5351 (1997).
[26] C. R. Scullard and R. M. Ziff, Phys. Rev. E **73**, 045102(R) (2006).
[27] X. M. Feng, Y. J. Deng, and H. W. J. Blöte, Phys. Rev. E **78**, 031136 (2008).
[28] I. Syozi, in *Phase Transitions and Critical Phenomena*, edited by C. Domb and M. S. Green (Academic, New York, 1972), Vol. 1.
[29] R. M. Ziff (private communication).
[30] The corresponding expression, Eq. (4) in [24], for the critical frontier contains a typographical error, missing a factor $(w+6)$ in the fourth term.
[31] C. R. Scullard, Phys. Rev. E **73**, 016107 (2006).
[32] I. Kondor, J. Phys. C **13**, L531 (1980).
[33] R. M. Ziff, Phys. Rev. E **73**, 016134 (2006).
[34] T. Utiyama, Prog. Theor. Phys. **6**, 907 (1951).
[35] R. Parviainen, J. Phys. A **40**, 9253 (2007).